Earth and Planetary Science Letters 400 (2014) 54–65

Contents lists available at ScienceDirect

Earth and Planetary Science Letters

www.elsevier.com/locate/epsl

Moon, Mars, Mercury: Basin formation ages and implications for the maximum surface age and the migration of gaseous planets

Stephanie C. Werner

Centre for Earth Evolution and Dynamics (CEED), University of Oslo, Norway

ARTICLE INFO

Article history:
Received 17 June 2013
Received in revised form 22 March 2014
Accepted 14 May 2014
Available online 4 June 2014
Editor: C. Sotin

Keywords:
Mars
Moon
Mercury
basin formation ages
earliest planetary evolution

ABSTRACT

Basin formation ages for Moon, Mars and Mercury are determined by cratering statistics, compared and evaluated with respect to their maximum surface ages and available isotope ages, and two possible Solar System evolution models. Both Mars and Mercury appear to have undergone significant resurfacing, so that at least the first 200–400 million years are not recorded on their surfaces. Basin frequency and crater frequencies below 150 km indicate that the Moon has the oldest surface, Mercury has an intermediate age, and Mars has the youngest preserved terrain. An offset between the basin size-frequency distribution, the smaller crater size-frequency distribution and the main belt asteroid size-frequency distribution is observed in all three cases, suggesting an age difference of about 150 Ma between basin and smaller crater distribution-based ages. I interpreted this in terms of lack of understanding of the basin formation process, and suggest that one possible explanation for the apparently under-representative basin frequency could be a different (lower) average impact velocity compatible with the 'Nice' flux model. The basin formation pattern derived with the standard monotonically decaying or the sawtooth-like Nice-model flux does not reveal a coherent picture according to the late heavy bombardment idea. This is here attributed to an incomplete understanding of the cratering rate ratios between the planetary bodies considered here. Because of the Moon's unique formation history, I also suggest that it is questionable whether the Moon is a suitable analogue for the formation, evolution and cratering record of the other terrestrial bodies.

1. Introduction

How old is the oldest surface on each of the terrestrial planets? This is one of the key issues of investigating the earliest phase of intense planetary bombardment, because the highest crater frequencies recorded on these planetary surfaces can be used to calculate their absolute model ages. When the surface of a planetary body becomes stable enough to accumulate remnants of its bombardment in the form of craters, then mixing and redistribution of material is limited to its surface and upper crust. This stage could mark the transition from planetary formation (accretion) to planetary differentiation and crustal evolution, and subsequent geological evolution (Albarede, 2009; Wood and Halliday, 2010). In the cases of Earth (due to plate tectonics) and Venus (due to recent resurfacing, for example by continuous global volcanism and/or global crustal overturn), the surface record of the earliest bombardment has been erased, and only isotopic data allow estimates of early-Earth's evolutionary stages. Therefore, I will examine here only Mercury, Mars and the Moon, and compare their record of large impact basins, considered to have formed only during the earliest phase of planetary evolution.

Some information of this earliest phase of planetary formation and transition to planetary evolution can be derived from meteorite isotope ages and lunar returned samples (summarized for example by Elkins-Tanton et al., 2011 for the Moon). The Earth's, Moon is suggested to have formed only 50–100 Ma after formation of the Solar System and to mark the end of Earth's accretion (Wood and Halliday, 2010). Such core segregation/formation ages do not necessarily date the formation of the first and/or last solid surface of these bodies. Planetary bodies were further bombarded in their accretion phase (Albarede, 2009; Wood and Halliday, 2010), but their surfaces may remain unable to record the bombardment in the form of crater and basin morphology. However, compositional differences may remain. Only a few lunar meteorites have been found, which date as early as 4.35 ± 0.15 Ga. As an example, the crystallization age of possible cryptomaria basalt of Kalahari 009 suggested by U–Pb dating of phosphates (Terada et al., 2007; Shih et al., 2008) falls within this period. The oldest crystallization

E-mail address: Stephanie.Werner@geo.uio.no.

http://dx.doi.org/10.1016/j.epsl.2014.05.019
0012-821X/

age determined for returned material from the Moon is about 4.46 ± 0.04 Ga (Norman et al., 2003; Nyquist et al., 2006).

The timing of the transition between early accretion and planetary evolution is related to the rate of internal heat loss, and is expected to be quicker on smaller bodies, but even the smallest of our bodies of interest, the Moon, show an extended period of magmatism (Shearer and Floss, 2000). The earliest phase of bombardment is often cited to have eliminated the earliest rocks, and with it the chronological information on the early differentiation (Basaltic Volcanism Study Project, 1981).

2. Concepts of the early bombardment phase

A correct time-frame for the formation phase of our Solar System based on impact flux data would provide a detailed and temporally-calibrated description of the early planetary geological evolution of all terrestrial bodies. This principle was first proposed by Öpik (1960). There exist different interpretations about the earliest bombardment history. One is based on crater counts of lunar surface units of known absolute isotope ages, from which the flux is then extrapolated into the more distant past, implying a static orbital evolution model for the planets since their formation. An alternative concept suggests a dynamic orbital evolution of the Solar System, and is termed the 'Nice' model. This orbital evolution model describes early orbital changes for the gaseous giant planets that have strong implications for orbital changes of the surviving planetesimals (Gomes et al., 2005; Tsiganis et al., 2005). This model has been suggested as a self-consistent explanation for the so-called Late Heavy Bombardment of the terrestrial planets, a spike in the inner-planets' bombardment rate originally proposed to occur at about 3.9 billions of years (Ga) ago, and originally postulated from isotope analysis of returned lunar samples (Tera et al., 1973, 1974). The Nice model challenges the assumption of monotonic cratering rate decay for the period following planetary formation, which has commonly been used for cratering-statistics based planetary surface-age determination (e.g., Shoemaker et al., 1963; Baldwin, 1971; Hartmann, 1972; Neukum et al., 1975). Recent updates modified the numerical Nice model to include observational constraints (Bottke et al., 2012; Morbidelli et al., 2012): the bombardment history of the Moon derived from the static and the dynamic model now concurs for times of about 4.1 Ga and younger, the period which is best constrained in the relation of crater frequency versus age. That implies that the original flux spike at ca. 3.9 Ga (Tera et al., 1973, 1974) has a much broader peak than hitherto recognized (Fassett and Minton, 2013), and both models have now similar flux decay for projectiles forming craters larger than 20 km. The extrapolation of the Nice model to smaller craters differs from the standard model by a factor of 2 to 4, depending on which shape of the crater size-frequency distribution is assumed. Prior to 4.1 Ga, some differences between these two concepts remain, but fewer observational constraints exist. How these two views influence our interpretation of the earliest geological evolution of the planets is discussed here, deduced from the cratering records of Mars, Moon and Mercury.

2.1. Constraints from isotope geochemistry and resultant ages

Dauphas and Pourmand (2011) suggested that Mars could have formed within only 2–4 Ma of the origin of the Solar System. Their results imply that Mars grew before dissipation of the nebular gas, when planetesimals (such as the parent bodies of chondrites) were still being formed. Other age information (e.g. Debaille et al., 2007, and for a review see Mezger et al., 2013) available for Mars suggests that Mars is slightly younger than the period between 4.54 to 4.46 Ga (Weirich et al., 2010; Bogard and Garrison, 2009; Bogard, 2011), in which frequent collisions among the planetesimal parent bodies occurred. Whether Mars is a left-over planetary embryo (including magma ocean crystallization and cumulate overturn) or has undergone a more extended accretion process remains unclear from the numerical models (Brasser, 2013; Mezger et al., 2013). However, no felsic (anorthosite) crust seems to be preserved on Mars. The oldest rock linked to Mars was thought to be the meteorite ALH84001, which has been recently re-dated to have crystallized only about 4.1 Ga ago (Lapen et al., 2010; Bouvier et al., 2009), but earlier estimates were closer to the formation age of the Solar System (e.g. Nyquist et al., 1995). Although debated, Pb–Pb ages derived by Bouvier et al. (2008, 2013) imply that the group of depleted shergottites now represents the oldest material known from Mars with an age of about 4.3 Ga, and the group of 'enriched' and intermediate shergottites are of the same age as the meteorite ALH84001, and about 4.1 Ga old. The apparently younger crystallization ages for the class of shergottites are more commonly accepted, and range between 173–596 Ma (Mars Meteorite Compendium), with the oldest age found for Tissint (Brennecka et al., 2012). The recently discovered Martian meteorite NWA7533 contains zircon grains, which could have formed as early as 4.428 ± 25 Ga ago (Humayun et al., 2013). The first in situ age determination on Mars revealed an age of 4.21 ± 0.35 Ga for the mixed detrital and authigenic components of a mudstone (Farley et al., 2013). Both ages indicate that Mars probably had a solid crust earlier than current cratering statistics allow determining.

The Moon is the most accessible and best studied terrestrial body beyond Earth, and potentially preserves a surface-geological record for nearly the entire 4.56 billion years of Solar System history. Studying the record of large impact basins and modelling their formation ages allows the description of the heavy bombardment period on three different bodies, Moon, Mercury and Mars, which are considered to show surfaces that witness the possible latest phase of planetary formation. Planetary formation models suggest that the terrestrial planets formed more or less at their current orbits from a narrow mass annulus (Hansen, 2009), in agreement with the Nice model (Walsh et al., 2011). It is thereby assumed that at least the inner Solar System bodies have experienced similar bombardment histories since planetary formation. As a first order assumption, I will make use of a cratering chronology concept that considers monotonic cratering rate decay, by extrapolation of crater counts of lunar surfaces of known isotope ages into the more distant past based on an implicitly presumed quasi-static orbital evolution model. This model has been shown to successfully describe both the static orbital evolution model and the dynamic evolution due to the migration of the gaseous planets for a period of about 4.1 Ga and younger (Werner et al., 2011; Morbidelli et al., 2012).

The cratering-rate ratio used to transfer the cratering chronology of Moon to other inner Solar System bodies has been derived from the observed set of planetesimals found in the asteroidal main belt and the population that has developed to planet-crossing orbits and potentially to projectiles that could impact the Earth–Moon system, Mercury or Mars today (Ivanov, 2001, 2006; Neukum et al., 2001b). The assumption is made that this cratering-rate ratio of today is applicable in the past and is well-determined. It has repeatedly been suggested that with time both the impact population has changed (e.g., Strom et al., 2005; Fassett et al., 2012a), and the dynamic orbital evolution of the Solar System has modified the orbits of the projectile population. This implies different source regions and different impact velocities (Tsiganis et al., 2005; Gomes et al., 2005; Morbidelli et al., 2005), or a combination of these. Little is known of the first few hundred million years after formation of the Solar System, and both planetary evolution models have been debated in favour of one or the other (e.g., Hartmann, 1975, 2003; Cohen et al., 2000;

Stöffler and Ryder, 2001; Chapman et al., 2007; Hartmann et al., 2007).

In this paper, I compare the formation ages of the large impact basins of the Moon, Mercury and Mars, either determined here or derived from previous publications. The set of production functions and chronology models used here primarily implies that the bombardment rate has monotonically declined during the heavy bombardment period, and the projectile population was the same for Mars, the Earth–Moon system and Mercury. In addition it is assumed that the shape of the time-averaged crater-production distribution has not changed over time, with the exception of basin-forming projectiles, and the cratering-rate ratio has been stable throughout time. The applicability of such an approach will be discussed, with respect to the following questions. How old are the oldest surfaces of the Moon, Mars and Mercury? What evidence remains of a (late) heavy bombardment on the planetary surfaces? Did the period(s) of heavy bombardment happen synchronously?

3. Characteristics of the basin formation age distribution of Mars, the Moon, and Mercury

Determination of basin formation ages is based on superposed impact crater populations. These age distributions and the basin populations themselves are used here to address the question of whether the bombardment history on the three bodies was synchronous, and whether the surviving surface represents similarly old phases of planetary evolution. For all three bodies, the ages of impact structures with diameters roughly larger than 250 km in diameter have been determined. For brevity, these structures will be called basins. The spatial distribution of all basins of Mars, the Moon and Mercury evaluated in this study are shown in Fig. 1. The datasets shown in Fig. 1 are not necessarily complete, but the selection criteria are similar. The formation ages of these basins are based on the statistics of superposed craters counted on the ejecta blanket units (or equivalent), and the crater sizes used for the age determination are at least above 50 km in diameter. The basin age distributions are given with respect to absolute model ages, additional scales in cumulative crater frequencies at different reference diameters (e.g. 300 km, 50 km, and 1 km) are given as well. Using these reference diameters already imply some assumptions of the behaviour of the size-frequency distribution used for the extrapolation beyond 50 km towards smaller crater diameters, i.e. 1 km.

3.1. Martian basins

The formation ages of martian basins have been investigated by Werner (2005, 2008) and extended for this paper. Frey (2006, 2008) postulated a number of basins with subdued topographic expressions (quasi-circular depressions, QCDs) and concluded, based on crater statistics, that they are older than the ones still topographically well exposed on the Martian surface. Fig. 2 shows a summary of age–frequency relations of visible (after Werner, 2008, ages are recalculated based on Ivanov's, 2001 chronology model), subdued basins (after Frey, 2008), and basins additionally dated in this work. For comparison purposes, the cumulative frequency for craters equal to and larger than 300 km (N_{cum} (300 km)) reported by Frey (2008) is recalculated here with the set of equations for the chronology model and the crater production function as suggested by Ivanov (2001). These recalculated ages are different from those that Frey (2008) derived.

The formation ages of the basins Hellas, Argyre, Isidis, and Chryse are used from the Werner compilation, while ages for Acidalia and Utopia are adopted from Frey's data set. Recalculated age values for Hellas, Argyre, Isidis, and Chryse based on the Frey (2008) data are significantly older compared to ages derived by

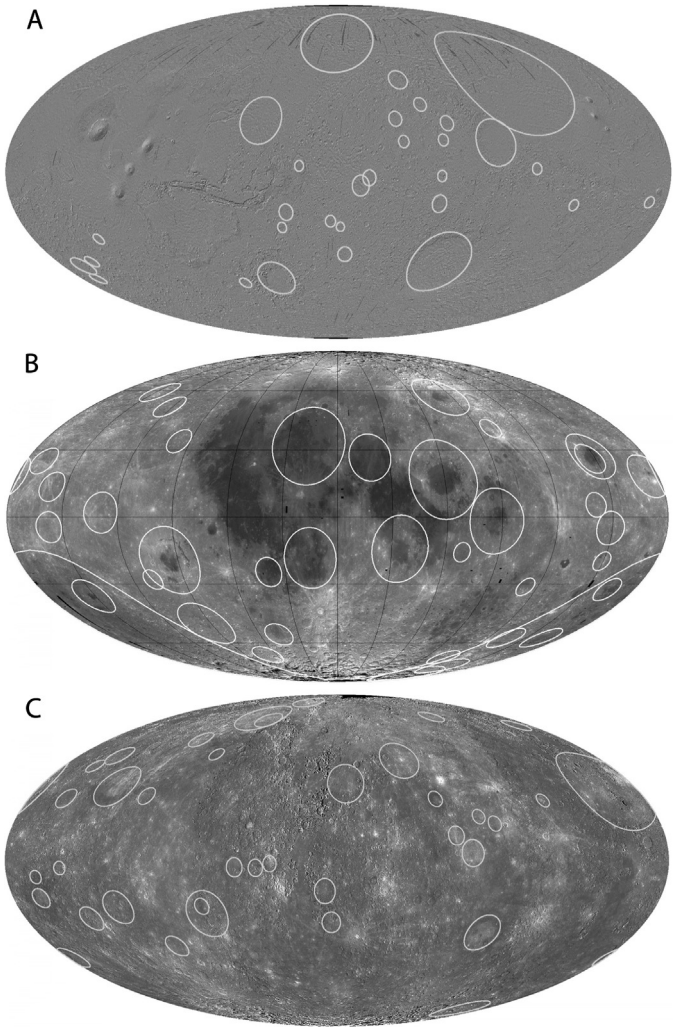

Fig. 1. The spatial distribution of basins used in this study for (A) Mars plotted over MOLA topography data, (B) Moon plotted over Clementine image data and (C) Mercury plotted over the Messenger image mosaic.

Werner (2008) and ages reported for Hellas, Argyre and Isidis (e.g., Fassett and Head, 2011). The ages determined by the latter two studies are almost identical after adopting the absolute model ages (Werner, 2008) by the chronology model of Ivanov (2001). Therefore, ages derived after Frey (2008) for Acidalia and Utopia (and other QCDs) may be significantly overestimated, and given the fact that they are devoid of long-wavelength magnetic anomalies, younger ages may be more reasonable as discussed by Werner (2008). Fig. 2 shows the entire compilation of the basin formation age distribution for Mars. There is no overlap of the formation-age ranges between the visible (morphologically defined) basins and the ones recognized with subdued topography, and this may cast doubt on the reliability of QCDs detection and their ages.

3.2. Lunar basins

Data used to investigate the temporal distribution of lunar basins are derived from Wilhelms (1987) and Neukum (1983) and are compared with the most recent results of Fassett et al. (2012a). The latter results are based on counts on the annular ejecta blanket units of basins larger than about 250 km. All ages are either refitted or recalculated for modern crater size-frequency distribution functions (as demonstrated in Werner, 2008) or new fits were performed on the original size-frequency measurements provided by Fassett et al. (2012a). For the latter I used only craters larger

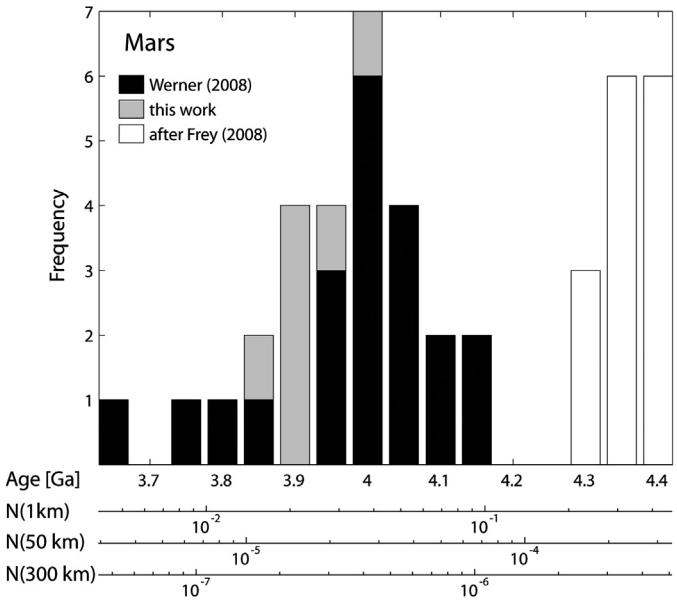

Fig. 2. The age distribution of Martian basins larger than about 250 km, according to work by Werner (2008), Frey (2008) and a few additional basins measured in this work. The cumulative crater frequency value N (300 km, 50 km, and 1 km) scale is given in accordance with the cratering chronology model and the crater size-frequency distribution from Ivanov (2001).

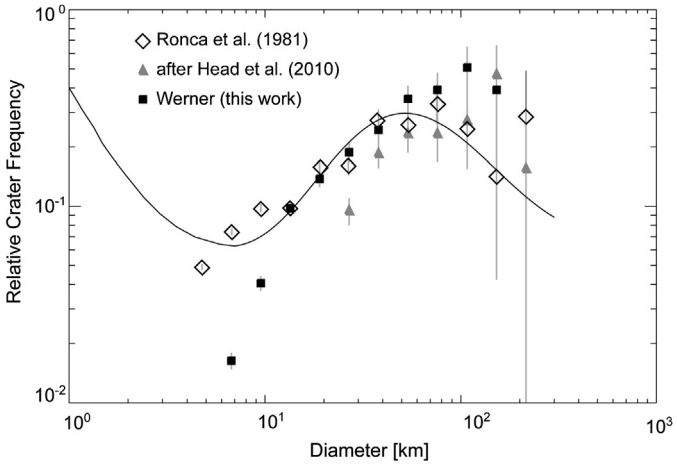

Fig. 3. Comparison of the crater size-frequency measurements by Ronca et al. (1981), Head et al. (2010) and my own measurements of an area photographed by the Zond 8 satellite. The region on the far-side of the Moon stretches between 170° E–140° W (in total 50°) and between 10°–30° S. My measurements are based on Kaguya and LOLA topographic data complemented by Clementine image data. The distribution scatters largely for craters larger than 100 km, but Ronca et al. (1981) and my measurements agree down to 15 km, while observations by Head et al. (2010) significantly underestimate crater frequencies below 50 km diameters. The solid line represents the lunar crater production function by Ivanov (2001).

than 50 km in diameter. Fassett et al. (2012a) used the LOLA-based spatial crater data set, which was first published by Head et al. (2010). As demonstrated in Fig. 3, this data set appears insufficiently accurate. This is probably due to the resolution limit related to the track density and cross-track interpolation. Fassett et al. (2012a) updated the LOLA data set for their study, and confirmed that the crater diameter range below 50 km appears to show strong signs of resurfacing activity (Fassett et al., 2012a; Hartmann, 1995). This is judged by the shape of the crater size-frequency distribution and evaluation of image data. However, Fassett et al. (2012a) convincingly show that the observed crater density of superposed craters is higher than that from the data collected by Wilhelms (1987). In cases when measured by both, the results by Fassett et al. (2012a) are in agreement with measurements reported by Neukum (1983), and also for the diameter range above 50 km (Fig. 3). Frey (2012) detected a substantial number of subdued lunar basins, using both topographic and gravity data. A similar study by Featherstone et al. (2013) confirms a great number of these basin candidates, suggesting 66 distinct basins, including the named ones. However, the latest data collected by the GRAIL mission confirms only Wilhelms' (1987) list of basins (Neumann et al., 2013). For the four data sets used in this lunar compilation, all absolute model ages are (re)calculated for a homogeneous comparison using the equations by Ivanov (2001). Fig. 4 shows three combinations of the resulting lunar basin formation age distributions.

3.3. Mercurian basins

For Mercury, I undertook new crater size-frequency measurements for 37 basins. The spatial distribution of these basins is shown in Fig. 1c. I have recognized similar basins as Fassett et al. (2012b). Their number of total basins is slightly higher; my independent mapping here confirms their certain basin candidates but disagrees on some of their probable candidates. Generally, the morphology of the basins (Fassett et al., 2012b) marked as probable candidates is very subdued, and reliable constraints will require the aid of detailed topographic or gravity data, which is not yet available globally. For the counts, I have prepared a global crater database, using a 250 m/pxl global mosaic (version 6 from http://messenger.jhuapl.edu/the_mission/mosaics.html.) The crater database is extended compared to that used by Herrick et al. (2011), mainly due to better image resolution with respect to the diameter range (here down to 1.5 km, with the smallest craters around 600 m in diameter), but also because of extended coverage compared to the flyby-mosaic used in their study. (The database can be provided upon request.) The units outlined for counting and basin formation age determination cover roughly an annulus of the width of up to one basin radius around the basin, because continuous ejecta blankets extend about one crater radius from the crater rim (Moore et al., 1974), and they are sufficiently thick to cover earlier formed craters. Therefore, the ejecta blanket is appropriate for dating the impact event itself. The same approach has been used in many other studies (e.g., Fassett et al., 2012a, or Werner, 2008). However, a clear outline of the ejecta blankets cannot always be provided. At first, all craters within the ejecta annulus were extracted from the database for each basin, and were subsequently verified visually as to whether these craters superpose or are buried by the ejecta blanket. Ages are determined mostly at diameter ranges larger than about 50 km in diameter, because at smaller crater diameters, resurfacing processes have modified the crater size-frequency distribution on the ejecta blankets. Detailed data can be requested from the author or see Appendix A, Fig. A. Fig. 5 summarizes the formation age distribution for Mercury.

3.4. The basin formation age distributions of Mars, the Moon and Mercury

Here I compare the temporal distribution of basins of the three investigated bodies, and focus on the flux estimates for the largest basin-forming bodies and the superposed craters of diameters larger than about 50 km. Although it is unclear whether the lunar basins were formed as a result of a spiking or rapidly declining bombardment rate, and whether this observation is restricted to the Earth–Moon system or is observable throughout the inner Solar System, I first assume that Solar System bodies have undergone similar impact histories since planetary formation, and the cratering rate has monotonically declined. The last basins formed represent a temporal marker-horizon, as first suggested by

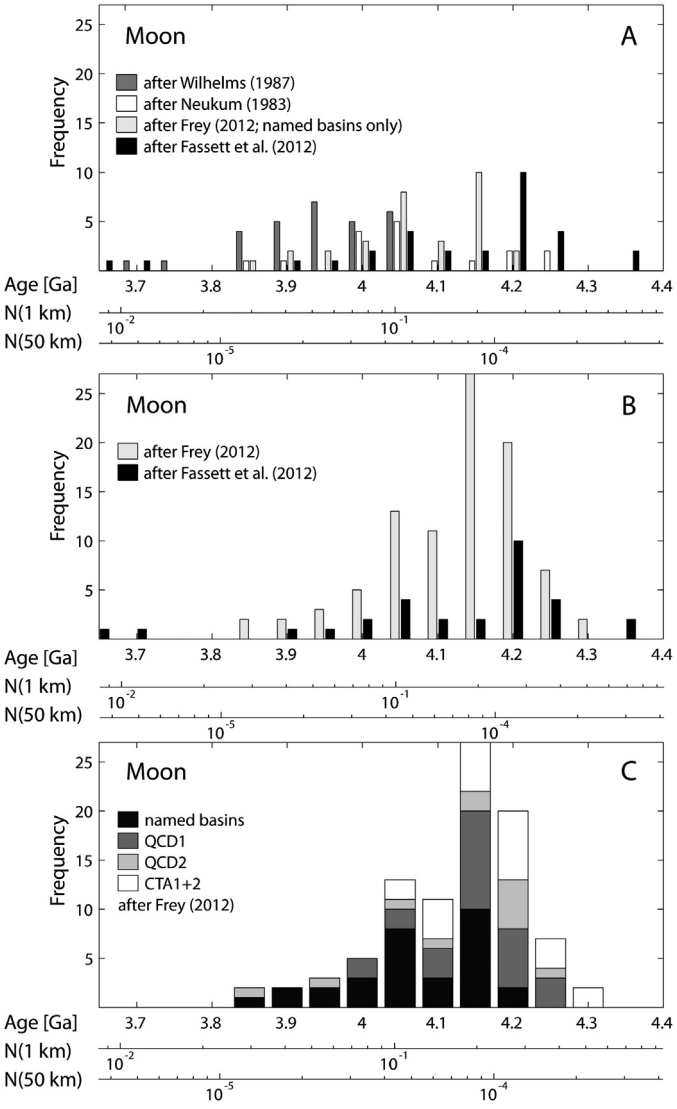

Fig. 4. (A) Basin formation ages for the Moon compiled from Neukum (1983), Wilhelms (1987), Fassett et al. (2012a) and named basins after Frey (2012). Only the three latter sets cover all named basins. (B) Formation ages derived from Fassett et al. (2012a) and all possible basins as detected by Frey (2012). (C) Detailed compilation of all different categories of basin candidates detected by Frey (2012). All basin formation ages are given for the combination of the crater size-frequency distribution of Ivanov (2001) and the chronology model of Neukum et al. (2001a), originally published by Neukum (1983).

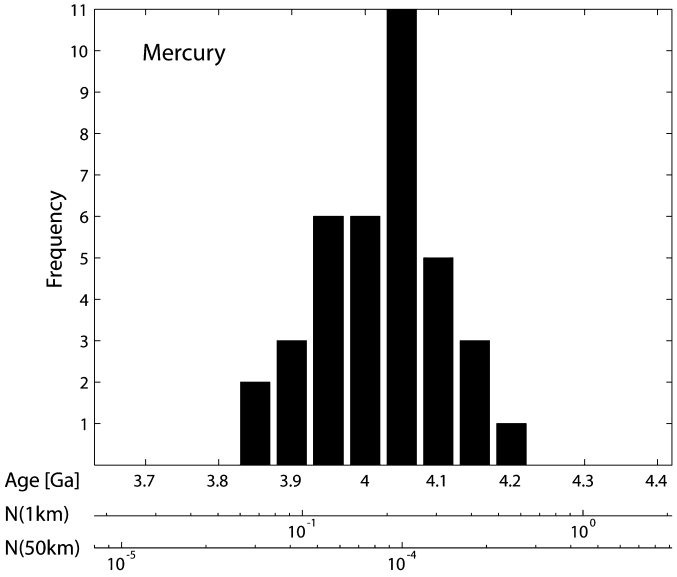

Fig. 5. The basin formation age distribution of Mercury. All ages are given for the combination of the crater size-frequency distribution and the chronology model of Neukum et al. (2001b).

Wetherill (1975). The same set of equations has been adopted for these three bodies (Ivanov, 2001, 2006; Neukum et al., 2001b) to present crater densities and absolute model ages for all three bodies, and the results are discussed here:

Martian basins formed between 3.5 and 4.15 Ga when considering only topographically and morphologically well constrained basins (Fig. 2). These ages, however, will need revision in the future according to Werner et al. (2014), which will shift the absolute basin age distribution some 100–200 million years towards older ages. The age distribution of these 28 basins appears to peak around 4.0 Ga. Including basin candidates (additionally 15) as suggested by Frey (2008), the formation age range is extended to as early as 4.4 Ga, and with a period of quiescence between 4.15 and 4.3 Ga when no basins formed. Werner (2008) pointed out that for some basins such as Flaugergues or Ladon (compare basin list by Tanaka et al., 1992, and not discussed by Frey, 2006), reliable ages cannot be determined due to substantial resurfacing processes. These basins are situated in the heavily cratered highlands with an average age of about 4.15 Ga (Werner, 2008), and could be as old as the highland units themselves (about 4.15 Ga). However, the formation gap probably relates to the different methods of how the basins and superposed craters are recognized, rather than being a real observation. For further discussions, I will exclude the basins proposed by Frey (2008) with the exception of the Acidalia, Utopia, Flaugergues and Ladon basins. The comparison between the Moon, Mars and Mercury, for the Martian surface, will rely on 30 basins, but four have no well defined ages making up the four oldest basins in these statistics.

Lunar basins are the best studied among basin distributions. Formation ages are compiled from Neukum (1983), Wilhelms (1987), Fassett et al. (2012a), and named basins are after Frey (2012). Only the three latter sets are complete with respect to the number of named basins. All sets jointly suggest that the lunar basins formed between 3.65 and 4.35 Ga (Fig. 4a), while the ages calculated after Fassett et al. spread over the largest period. Formation of basins after Wilhelms (1987), who found systematically lower crater densities superposing the ejecta blankets documented by Fassett et al. (2012a), cover only a period between 3.7 and 4.1 Ga. Frey (2012) has not only analysed crater densities superposing named basins, but also studied topographic and gravity data for subdued basin structures and suggests about 60 additional basin candidates, including their stratigraphic relationship derived from cratering statistics. The formation ages for these structures and the named basins are shown in Fig. 4c. Comparing the age distribution of the named basins (Fig. 4c), there are two peaks: one at 4.05 Ga and one at around 4.2 Ga. This observation relies only on 30 basins, and considering the basin candidates (Frey, 2012), this gap almost disappears (Fig. 4b). For further comparison, I will use the ages determined using the cumulative crater frequency data set derived by Fassett et al. (2012a) only, because these ages I determined directly from the measurements.

Mercurian basin ages for 37 basins were determined in this work. They appear to have formed between 3.8 and 4.2 Ga. The distribution demonstrates one peak at around 4.05 Ga (Fig. 5). The inferred absolute ages differ especially for Mercury in the different approaches (e.g. Neukum et al., 2001b; Massironi et al., 2009; Marchi et al., 2013). Chronology transfers based on de-biased flux estimates (after Bottke et al., 2002) result in lower absolute ages than determined here.

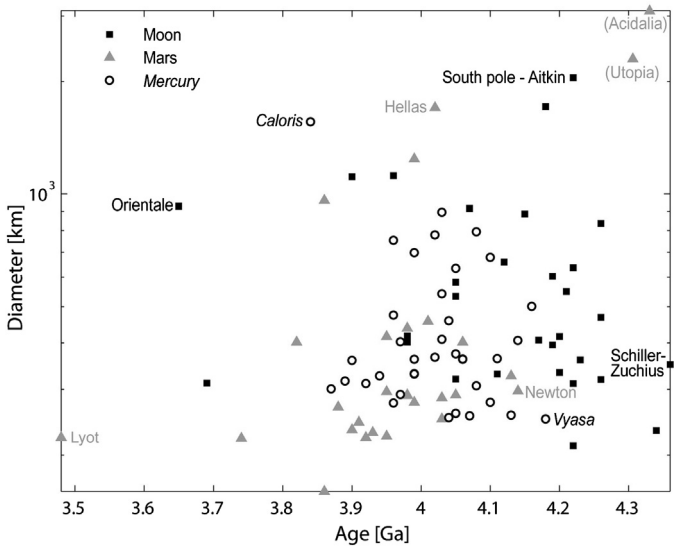

Fig. 6. The age–diameter relation for basins larger than about 250 km on Mercury, Moon and Mars. This relation is limited to the basins for which ages were determined and discussed in this work. For orientation, the youngest basins (Caloris, Orientale, and Lyot), the oldest basins (Vyasa, Schiller-Zuchius, and Newton) and the largest basins (Caloris, South Pole–Aitken, and for Mars Hellas, Utopia, and Acidalia) are indicated by their names.

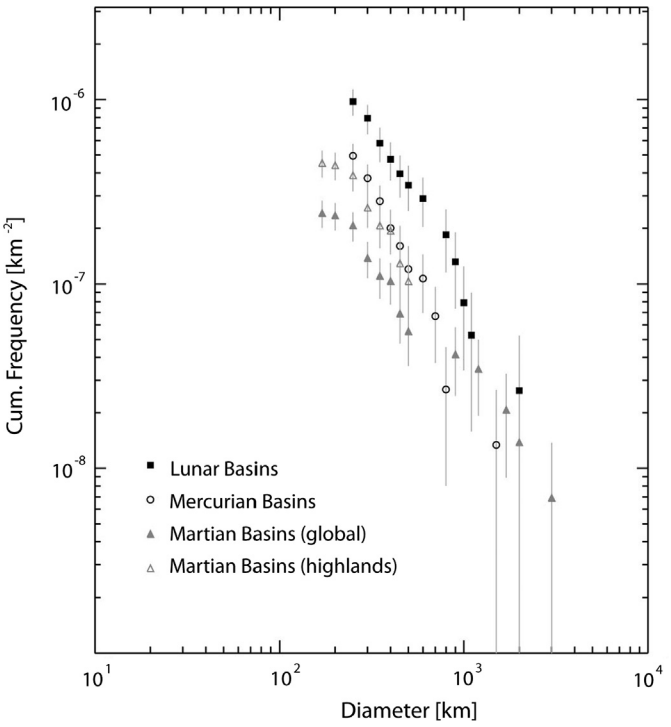

Fig. 7. Size-frequency distribution of basins larger than about 250 km in diameter of Moon, Mars and Mercury. Martian basin frequencies are represented normalized to the area of global Mars (solid symbol), and additionally, frequencies of basins between 850 and 250 km in diameter are normalized for highland area only (empty symbol), the unit, in which they are found.

3.5. Age–diameter relations and basin size-frequency distributions

For further evaluation of the recorded early bombardment history on Mars, the Moon, and Mercury, I compare the three bodies in greater detail. First, I examine if the largest basin is the oldest or might be related to the late heavy bombardment period (e.g., Cadogan, 1974; Pieters and Head, 2001; Tera et al., 1973, 1974; Wetherill, 1975; Bottke et al., 2013). Fig. 6 summarizes the age–diameter relations for all three bodies. Diameters for the lunar basins were extracted from the Head et al. (2010) global crater database; I derived mercurian basin diameters from the global image mosaic, while martian basin diameters were derived from topographic data. For all three, the trend is that the larger basins are older, but in detail this correlation appears not well established. On Mars, however, both extremes, Lyot (smallest and youngest) and Utopia (largest and oldest) fulfil the postulated relation. On Mercury, the youngest basin is also the largest (Caloris basin). On the Moon, the youngest basin is the Orientale basin, and considering the outer most escarpments it is one of the largest basins. Quite a few basins have multiple rings, and it is unclear which of these escarpments actually form the basin's outer boundary, and which are tectonic deformations related to the basin formation. Therefore, this age–diameter relation may be obscured, as the outer escarpments may already be eroded. The largest basin diameter range is covered by martian basins, but size effects due to different gravity and impact velocities are not taken into account here.

The second obvious comparison is the basin size-frequency distribution itself. Fig. 7 shows the size-frequency distribution of basins larger than 250 km in diameter for the Moon, Mars, and Mercury. Both the Moon and Mercury record remarkably similar distribution patterns (as discussed also by Fassett et al., 2011, 2012b; Marchi et al., 2013), while on Mars a distinct drop is observed for basins smaller than about 850 km in diameter, assuming the entire basin population to be globally representative. For the Moon and Mercury, the basins can be considered to represent a global distribution, while for Mars part of the distribution is recorded only on highlands units, and thus the highland unit area size is considered for determining the basin density for basins smaller than 850 km as well. In Fig. 7, when treating only the larger diameter range representative for a martian global distribution, and calculated the frequency for basins smaller than 850 km with respect to the highland area (roughly half of the total martian surface) only, the basin size-frequency distribution appears more smooth. However, the martian basin size-frequency distribution appears to be differently shaped at diameters larger than 850 km compared with the Moon and Mercury.

Third, the total basin spatial density, for example given as a cumulative density for impact basins larger than 250 km diameter, is consistent with the inference that Moon has the oldest preserved crust, Mars the youngest and Mercury is intermediate (Fig. 7).

4. Discussion

This paper started out to address the questions of the maximum age of preserved surfaces of the Moon, Mars and Mercury, of evidence of a (late) heavy bombardment, and of a synchronous behaviour of the basin-forming projectile flux on these three bodies (given the current sets of models).

The derived absolute values of surface ages indisputably depend on the set of chronology models and crater-production functions used. The results may vary significantly. Werner and Ivanov (2007) outlined the uncertainties in the chronology model when different crater-production functions are used to calibrate the lunar chronology model, and these uncertainties increase after transfer to the other bodies. Significant absolute model age variations due to currently used crater statistics schemes may occur, e.g., as discussed for Mars (Werner and Tanaka, 2011). Cratering rate ratio uncertainties make the absolute age calibration beyond Moon challenging (e.g., Le Feuvre and Wieczorek, 2011). Here, I discuss the maximum surface age estimates based on a specific set of equations as outlined in the different sections. Thus, even the absolute age values only indicate a qualitative description. Therefore, all diagrams are plotted also with relative crater frequencies at the cumulative crater frequency values of N_{cum} (1 km) and N_{cum} (50 km).

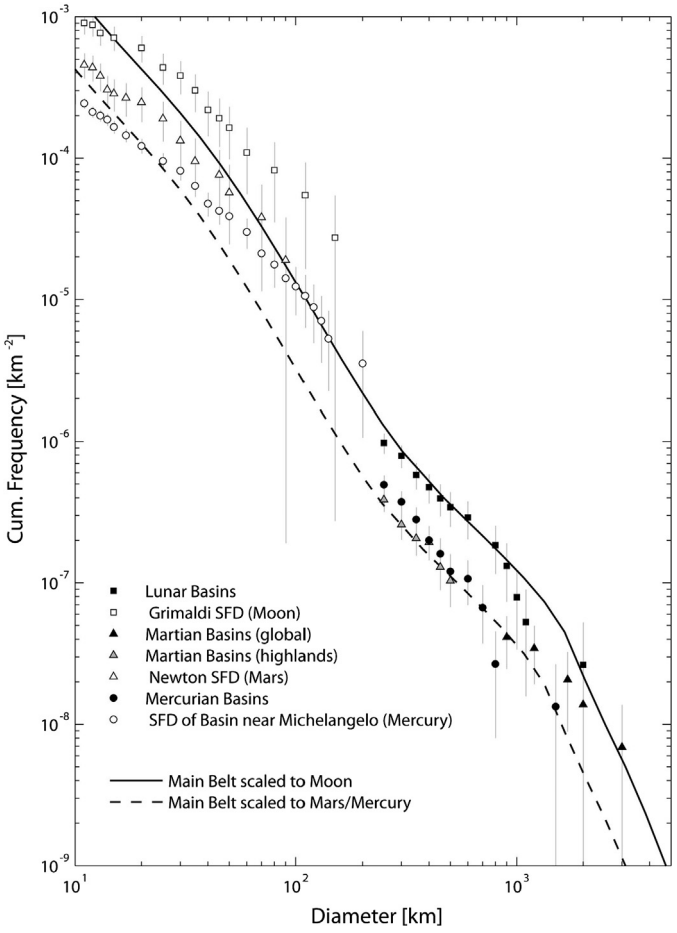

Fig. 8. Cumulative crater size-frequency distributions for Mars, Moon, and Mercury. Data for the basins as shown in Fig. 7, but in comparison with simple scaling of the Main Belt asteroid size-frequency distribution according to Bottke et al. (2005) and one example measurement of one of the oldest basins for each of the three bodies.

Fig. 8 shows the observed global basin size-frequency distribution for the Moon, Mercury and Mars, and for the latter the basins below 850 km in diameter are plotted proportionally to the highland area size, while all others are plotted with respect to the total global surface area. In addition to the size-frequency distributions of basins, one measurement example for one of the oldest surfaces units of each body is shown. Basin distribution and the measurements typical for the oldest surfaces are plotted together with main belt asteroid size-frequency distribution curves as suggested by Bottke et al. (2005), but scaled to the specific body. The main belt asteroid distribution is suggested (e.g., Strom et al., 2005) to best represent projectile population for the time period investigated here.

At least from the spatial number density of basins, the Moon has the oldest surface, while Mercury and Mars are younger. Based on current cratering chronology models that are derived from crater ranges below about 150 km in diameter, the maximum surface age for the Moon is about 4.3 ± 0.05 Ga (calculated here from crater density data by Fassett et al., 2012a), and 4.1 ± 0.05 Ga for Mars (Werner, 2008). The maximum surface age for Mercury is determined in this paper to about 4.1 ± 0.1 Ga (see also Marchi et al., 2013, but they use both a different cratering chronology model and crater production function). This is similar to Mars, but with larger statistical uncertainties.

The strongest resurfacing activity, however, is observed for Mercury, whose intermediate crater size-frequency distribution is modified significantly at ranges smaller than typically 75 km (Fig. 8). The resurfacing for Mercury appears to be of global extent (Marchi et al., 2013). On the martian highland units, craters smaller than about 50 km show signs of resurfacing, and craters below 15 km are significantly affected (Tanaka et al., 1992). Craters on the martian lowland units and volcanic provinces are affected across the entire crater diameter range. Interestingly, the cumulative frequencies of the basin distribution, however, result in fitted absolute surface model ages about 150 million years younger than the maximum surface age found with smaller crater diameters, with Mars being the youngest (Fig. 8).

Using a standard chronology, e.g., Neukum et al. (2001a), requires more than a doubling of the observed crater densities to overcome the difference of 4.3 Ga and the isotope age of 4.46 Ga for the lunar case. This apparent upper age limit could be due to the combination of the exponential nature of the early bombardment flux and crater-size related saturation, and net accumulation may be undetermined (e.g., Gault, 1970; Hartmann, 1984; Richardson, 2009), but a simple recalibration of the lunar cratering chronology model (Werner and Ivanov, 2007) could change the maximum surface age for the Moon, Mercury and Mars. Different flux evolution in concordance with the Nice model suggests a lower flux before 4.1 Ga than the standard cratering chronology model (e.g., Morbidelli et al., 2012). The Nice model requires a changing orbital configuration for the gaseous planets before 4.1 Ga, and yet lower crater densities are required to result in older surface ages. However, for this period no direct constraints on the absolute age–crater density link are available. This leads to the second question, as to whether the basin formation pattern suggests a basin-forming projectile flux that occurs on all three bodies synchronously. Keeping the uncertainties of the applied cratering chronology models in mind, the range of basin formation ages on all three bodies varies (Fig. 9), and apparent peaks occur at different times. Mars and Mercury show one peak each, although they are offset towards younger ages for Mars. The martian age peak, as well as the total range are broader in comparison to Mercury. The lunar basin age range is similar to Mars', but peaks at about 4.05 Ga (similar to Mercury) and again at 4.2 Ga, unlike any of the other two bodies. This second peak was interpreted by Fassett et al. (2012a, 2012b) as artificial due to impact saturation, because basin formation before 4.2 Ga was in a stage of equilibrium, thus, apparently erasing the earliest basin-superposing cratering record used for age determination here.

The spatial abundance of basins with time (Fig. 9b) roughly suggests similar basin-forming flux for all bodies for the period younger than about 4.0 Ga, when impact rate ratios according to Ivanov (2001) and Neukum et al. (2001b) are used. Different cratering rate ratios, such as those based on the de-biased planet-crossing asteroid model of Bottke et al. (2002), result in younger ages for Mercury, but the double peak for the Moon would not disappear.

To evaluate the differences to the results of the two chronology models, I recalculated the basin ages using the Nice model for the Moon and Mercury (Morbidelli et al., 2012; Marchi et al., 2013). The different chronology models are defined at N_{cum} (1 km) and N_{cum} (20 km), respectively, I determined the ratio between N_{cum} (1 km) and N_{cum} (20 km) using the crater production function according to Neukum (1983), and the updated version of Neukum et al. (2001a, 2001b). The latter is used to illustrate the uncertainties inferred by the use of different production functions. It is important to note that the result depends on which crater production function is used and suggests a degree of caution. The comparison between the basin age distribution according to the standard chronology and the Nice chronology for the Moon and Mercury is shown in Fig. 10. With the two selected crater production functions, there is no synchronous behaviour observed using the Nice model. The cratering rate ratios of the utilised set of stan-

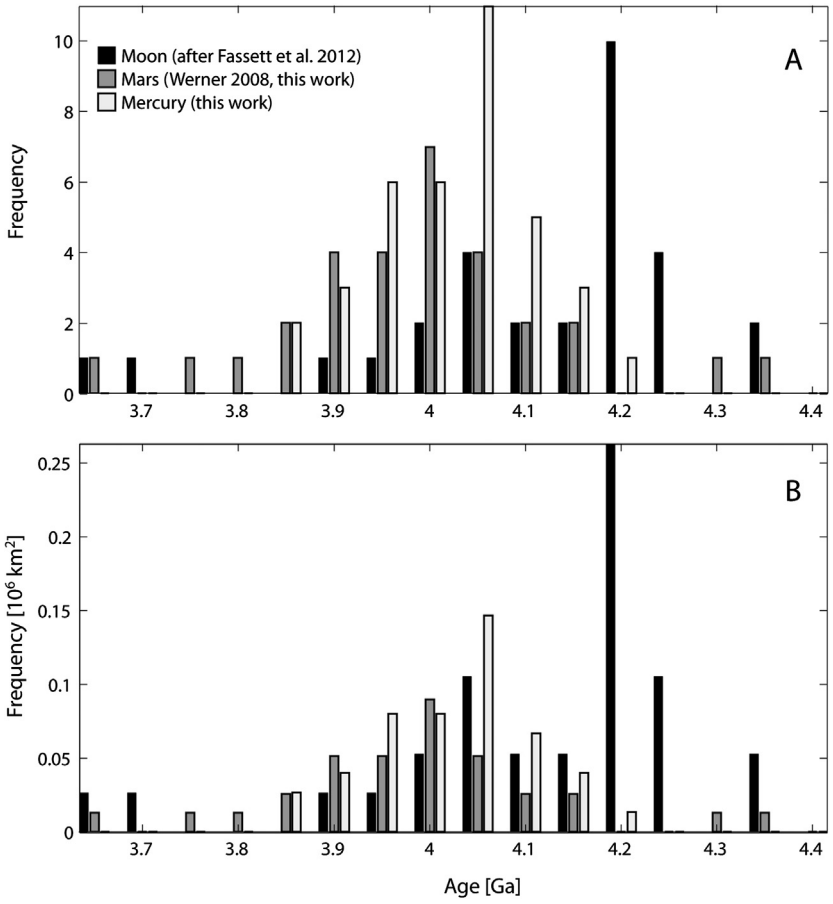

Fig. 9. Comparison of the basin formation age distribution of Moon, Mars and Mercury in absolute numbers (A) and scaled per 10^6 km^2 (B).

dard model equations differ from the Nice model, and it has been previously demonstrated to produce divergent results (e.g., Le Feuvre and Wieczorek, 2011).

Improved determination of the cratering rate ratios derived from observed asteroid catalogues, or *N*-body simulations of asteroids, may allow for shifts, although small-number statistics may prevent a more certain interpretation, and in the current setting, synchronicity cannot confidently be confirmed for either model approach.

5. Conclusion

In this study, basin formation-age ranges, the implied basin forming projectile flux, and the basin size-frequency distribution itself have been compared for the Moon, Mars and Mercury. The Moon appears to hold the oldest surface record. Mars and Mercury have undergone more intensive global resurfacing than the Moon, unless the cratering rate ratios used to calibrate the chronology models of Mercury and Mars are off by a factor of two to three. To overcome the age difference would require an order of magnitude of more craters on the surface of Mercury or Mars. Nevertheless, the smaller crater size-range modification and image interpretation indicates that Mercury globally underwent more intense resurfacing than the highland units of Mars, as also suggested by Strom et al. (2005) and Fassett et al. (2011). On Mars, however, widespread volcanic activity and the formation of the lowlands erased the entire crater record in these units, while resurfacing on Mercury appears to be a more global, and less important event (compare Marchi et al., 2013).

With the current chronology models and crater production functions for these bodies, basin formation appears at a similar time frame, if the standard model is used, but the detailed flux behaviour suggests that they occurred at different intensities (Fig. 9b). The differing cratering rate ratio of the Nice model flux for Mercury (Marchi et al., 2013) results in a shift of the basin formation age distribution for Moon and Mercury, such that no coinciding flux pattern is observed. One striking observation is that the maximum surface age derived from the basin distribution itself and that from the crater distribution of most densely cratered surface units at smaller crater diameters appears younger by about 150 million years for all bodies (Fig. 8). There is relatively good agreement of the directly observable size-frequency distribution for the main belt asteroids and the size-frequency distribution of basins (Fig. 8). Several studies suggest that the large crater distribution also resembles the main belt population, at least for the old surfaces (e.g., Strom et al., 2005). However, using simple continuous crater-projectile scaling, the observed frequencies of basins and craters are not coherent, as implied by the deviating size-frequency distributions of basins and large craters. Either the scaling relations for basins are not well understood, or this is the most important indication that the average impact velocity has changed during the basin forming period. (The large number of unstudied subdued basin features detected in gravity and topographic data may reduce the discrepancy. The recognition of circular depressions, however, is not limited to the basin range. However, for the Moon, latest gravity data collected by GRAIL could not confirm most of the QCDs.)

Evaluating the role of velocity variations requires improved descriptions of the crater size-frequency distributions, and target properties (e.g. presence of ice in the regolith) for crater scaling law adjustments. As demonstrated here, modified crater size-frequency distribution, but also new age estimates based on iso-

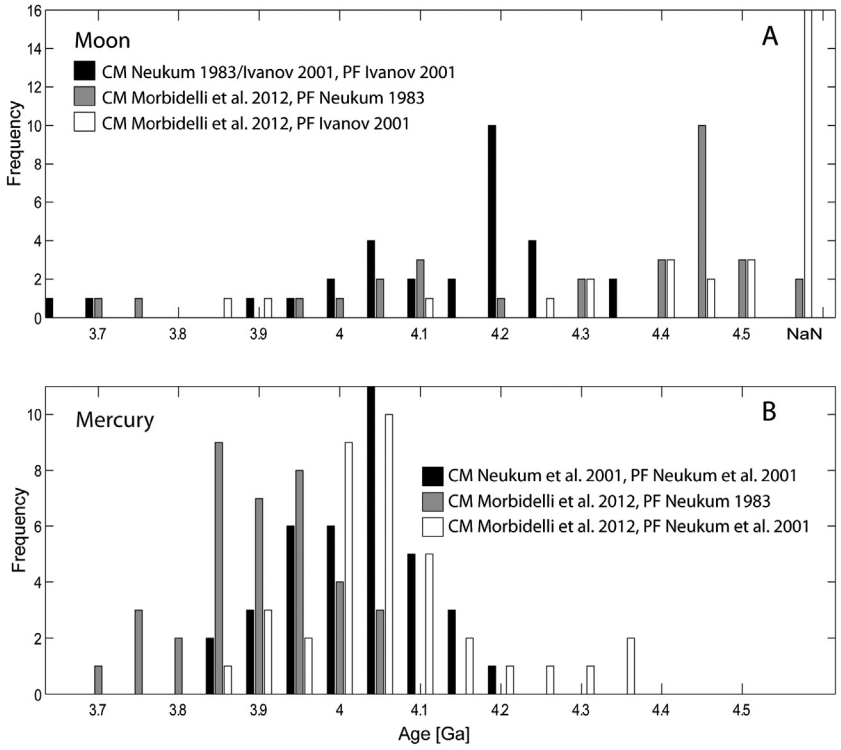

Fig. 10. The basin formation age distribution for the Moon and Mercury. The ages have been determined for a monotonic and for a sawtooth-like decaying flux. (A) Moon: All basin formation ages are given for the combination of the crater size-frequency distribution of Ivanov (2001) and the chronology model of Neukum et al. (2001a) as in Fig. 4, and the sawtooth-like decay (Morbidelli et al., 2012). The ratios between the N_{cum} (1 km) and N_{cum} (20 km) were calculated based on two crater production function models (Neukum, 1983; Ivanov, 2001). Basin ages, which result in ages beyond the age of the Solar System, are plotted in the column marked by 'NaN'. (B) Mercury: All basin formation ages are given for the combination of the crater size-frequency distribution and the chronology model of Neukum et al. (2001b) as in Fig. 5, and the sawtooth-like decay (Morbidelli et al., 2012; Marchi et al., 2013). The ratio between the N_{cum} (1 km) and N_{cum} (20 km) were calculated based on two crater production function models (Neukum, 1983; Neukum et al., 2001b). The comparison is valid only for the equivalent sets of equations and are highlighted in the same grey shade.

tope geochemistry, significantly changes the chronology models, and influences the synchronicity aspect, which also depends on the utilised cratering rate ratios. Dynamical planetary system evolution models imply additional variations in the average impact velocities with time. The relative importance of these uncertainties can only be unravelled by either sample return or the development of feasible in-situ age dating, and applied, for example, to Mars. This will provide an additional age calibration point beyond the Earth–Moon system.

6. Speculative epilogue

Absolute model ages derived from Hf–W–chronometry (e.g., Kleine et al., 2009; Dauphas and Pourmand, 2011) suggest that the Moon was delayed in its evolution by about 50 to 100 million years compared to Mars. Corresponding geochemical constraints are not available for Mercury due to the lack of samples. Surface absolute model ages based on cratering statistics, however, suggest that the lunar surface is the most ancient. With the Nice model flux behaviour, the maximum lunar crater density could be interpreted as equivalent to the maximum isotope ages derived for the Moon and lunar surface rocks (Werner et al., 2011; Morbidelli et al., 2012). In spite of the uncertainties in cratering rates, the maximum absolute surface model ages for Mercury and Mars are younger than for the Moon, and these planets experienced global resurfacing in their earliest history, indicated by different crustal composition (e.g., Nittler et al., 2011; Bandfield et al., 2000).

If Mars formed as early as 2–4 million years after the formation of the calcium- and aluminium-rich inclusions (CAIs, defining the zero age of our Solar System) that date the formation of the Solar System (Dauphas and Pourmand, 2011), no surface record of the first 400 million years (if ages are derived by the standard cratering chronology) or about 250 million years (according to Nice model fluxes) is preserved on Mars. A delayed global surface solidification and a different magma ocean evolution could provide an explanation, which may also have prevented the formation of a primary anorthositic crust on Mars and Mercury in favour of a more basaltic composition. Obviously, composition (Mg, Fe, Si), oxygen fugacity, as well as the size (inferred pressure and temperature range) of the body may play significant roles (Elkins-Tanton, 2012). However, an anorthositic crust has not been detected on Vesta (e.g., Thangjam et al., 2013), which is considered to have surfaces of at least 4.5 Ga as testified by ages found for howardite–eucrite–diagonite (HED) classes of meteorites (e.g., Kennedy et al., 2013). Therefore, the presence or lack of an anorthositic crust is not an indication of the absolute surface antiquity.

Perhaps the Moon's extraordinary formation (born from a battered mother Earth) makes its evolution and cratering record dissimilar from the evolution and cratering record to the other terrestrial bodies.

Acknowledgements

SCW thanks Caleb Fassett and an anonymous reviewer, as well as the editor Christophe Sotin for their helpful comments to improve the original manuscript, and Lewis D. Ashwal for improving the English. SCW appreciates funding from the Research Council of Norway through its Centres of Excellence funding scheme, project number 223272 (CEED), and from the European Research Council under the Union's Seventh Framework Programme (FP7/2007–2013)/ERC Advanced Grant Agreement Number 267631 (Beyond Plate Tectonics).

Appendix A

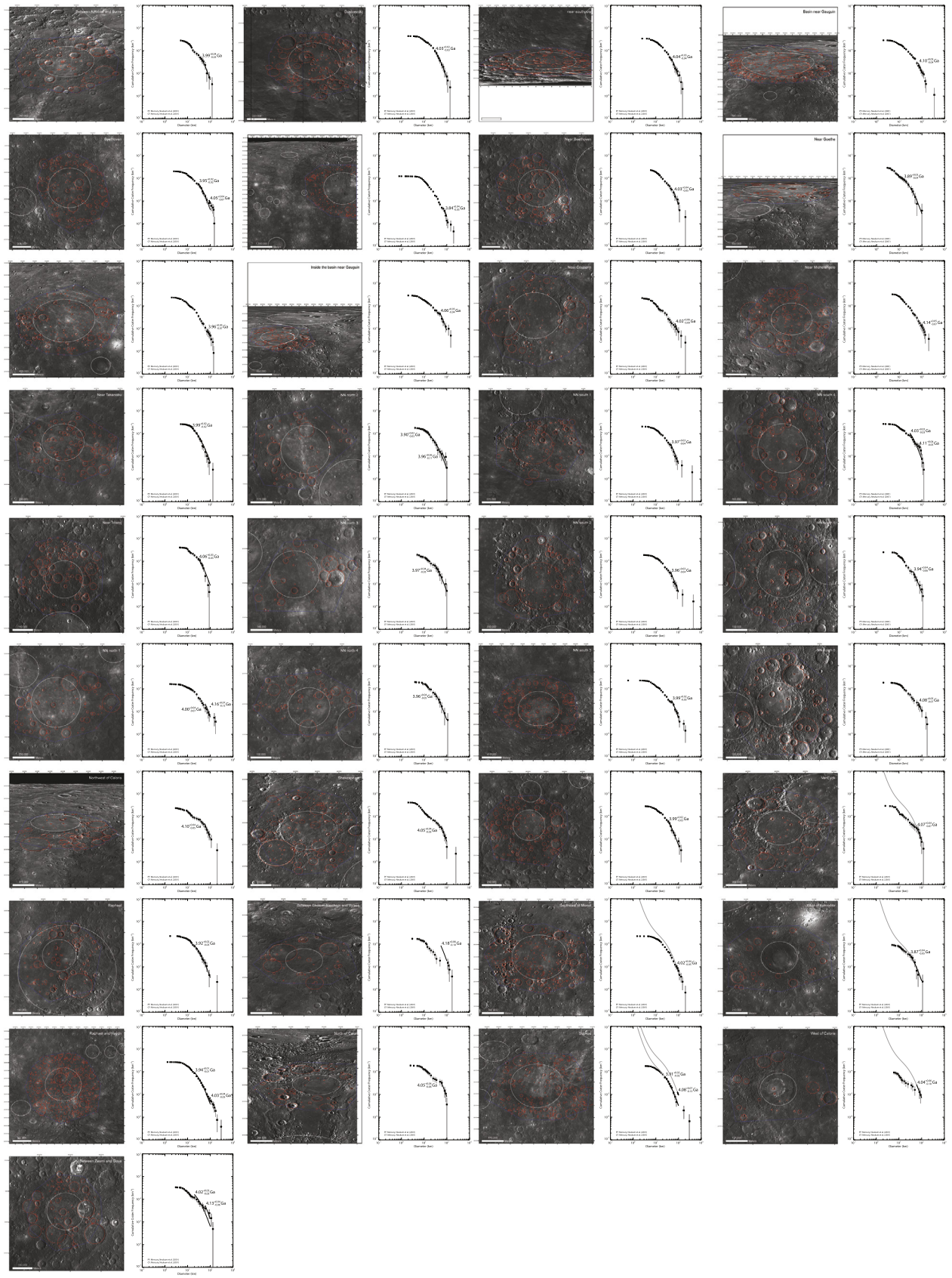

Fig. A. Thirty-seven Mercurian basins are shown. For each, the basin outline is white, superposed craters for age estimation purposes are outlined in red, and the counting unit is outlined in blue. The crater distribution is plotted as well as the age fit. If there are two ages given, the older is used. (For interpretation of the references to color in this figure legend, the reader is referred to the web version of this article.)

References

Albarède, F., 2009. Volatile accretion history of the terrestrial planets and dynamic implications. Nature 461, 1227–1233.

Baldwin, R.B., 1971. On the history of lunar impact cratering: the absolute time scale and the origin of planetesimals. Icarus 14, 36.

Bandfield, J.L., Hamilton, V.E., Christensen, P.R., 2000. A global view of Martian surface compositions from MGS-TES. Science 287, 1626–1630.

Basaltic Volcanism Study Project, 1981. Basaltic Volcanism on the Terrestrial Planets. Pergamon Press, Inc., New York. 1286 pp.

Bogard, D.D., 2011. K–Ar ages of meteorites: clues to parent-body thermal histories. Chem. Erde 71, 207–226.

Bogard, D.D., Garrison, D.H., 2009. Ar–Ar and I–Xe ages and thermal histories of three unusual metal-rich meteorites. Geochim. Cosmochim. Acta 73, 6965–6983.

Bottke, W.F., Morbidelli, A., Jedicke, R., Petit, J.-M., Levison, H.F., Michel, P., Metcalfe, T.S., 2002. Debiased orbital and absolute magnitude distribution of the near-Earth objects. Icarus 156, 399–433.

Bottke, W.F., Durda, D.D., Nesvorný, D., Jedicke, R., Morbidelli, A., Vokrouhlický, D., Levison, H., 2005. The fossilized size distribution of the main asteroid belt. Icarus 175, 111–140.

Bottke, W.F., Vokrouhlický, D., Minton, D., Nesvorný, D., Morbidelli, A., Brasser, R., Simonson, B., Levison, H.F., 2012. An Archaean heavy bombardment from a destabilized extension of the asteroid belt. Nature 485 (7396), 78–81.

Bottke, W.F., Marchi, S., Kring, D., 2013. On the formation age of South Pole–Aitken basin. In: Lunar Science Virtual Forum.

Bouvier, A., Blichert-Toft, J., Vervoort, J.D., Gillet, P., Albarède, F., 2008. The case for old basaltic shergottites. Earth Planet. Sci. Lett. 266, 105–124.

Bouvier, A., Blichert-Toft, J., Albarède, F., 2009. Martian meteorite chronology and the evolution of the interior of Mars. Earth Planet. Sci. Lett. 280, 285–295.

Bouvier, A., Blichert-Toft, J., Albarède, F., El Goresy, A., Agee, C.B., Gillet, P., 2013. U–Th–Pb evolution requires very old age for newly found depleted shergottites. In: 44th Lunar and Planetary Science Conference. In: LPI Contrib., vol. 1719, p. 2421.

Brasser, R., 2013. The formation of Mars: building blocks and accretion time scale. Space Sci. Rev. 174, 11–25.

Brennecka, G.A., Borg, L.E., Wadhwa, M., 2012. The age of Tissint: Sm–Nd and Rb–Sr isotope systematics. In: 75th Annual Meeting of the Meteoritical Society. In: Meteoritics and Planetary Science Supplement. Abstract No. 5157.

Cadogan, P.H., 1974. Oldest and largest lunar basin? Nature 250, 315–316.

Chapman, C.R., Cohen, B.A., Grinspoon, D.H., 2007. What are the real constraints on the existence and magnitude of the late heavy bombardment? Icarus 189, 233–245.

Cohen, B.A., Swindle, T.D., Kring, D.A., 2000. Support for the lunar cataclysm hypothesis from lunar meteorite impact melt ages. Science 290, 1754–1756.

Dauphas, N., Pourmand, A., 2011. Hf–W–Th evidence for rapid growth of Mars and its status as a planetary embryo. Nature 473 (7348), 489–492.

Debaille, V., Brandon, A.D., Yin, Q.-Z., Jacobsen, B., 2007. Coupled ^{142}Nd–^{143}Nd evidence for a protracted magma ocean in Mars. Nature 450, 525–528.

Elkins-Tanton, L., 2012. Magma oceans in the inner Solar System. Annu. Rev. Earth Planet. Sci. 40, 113–139.

Elkins-Tanton, L., Burgess, S., Yin, Q.-Z., 2011. The lunar magma ocean: reconciling the solidification process with lunar petrology and geochronology. Earth Planet. Sci. Lett. 304, 326–336.

Farley, K.A., Malespin, C., Mahaffy, P., Grotzinger, J.P., Vasconcelos, P.M., Milliken, R.E., Malin, M., Edgett, K.S., Pavlov, A.A., Hurowitz, J.A., Grant, J.A., Miller, H.B., Arvidson, R., Beegle, L., Calef, F., Conrad, P.G., Dietrich, W.E., Eigenbrode, J., Gellert, R., Gupta, S., Hamilton, V., Hassler, D.M., Lewis, K.W., McLennan, S.M., Ming, D., Navarro-González, R., Schwenzer, S.P., Steele, A., Stolper, E.M., Sumner, D.Y., Vaniman, D., Vasavada, A., Williford, K., Wimmer-Schweingruber, R.F., the MSL Science Team, 2013. In situ radiometric and exposure age dating of the Martian surface. Science B43 (6169). http://dx.doi.org/10.1126/science.1247166.

Fassett, C.I., Head, J.W., 2011. Sequence and timing of conditions on early Mars. Icarus 211, 1204–1214.

Fassett, C.I., Minton, D.A., 2013. Impact bombardment of the terrestrial planets and the early history of the Solar System. Nat. Geosci. 6, 520–524.

Fassett, C.I., Kadish, S.J., Head, J.W., Solomon, S.C., Strom, R.G., 2011. The global population of large craters on Mercury and comparison with the Moon. Geophys. Res. Lett. 38. CiteID L10202.

Fassett, C.I., Head, J.W., Kadish, S.J., Mazarico, E., Neumann, G.A., Smith, D.E., Zuber, M.T., 2012a. Lunar impact basins: stratigraphy, sequence and ages from superposed impact crater populations measured from Lunar Orbiter Laser Altimeter (LOLA) data. J. Geophys. Res. 117. CiteID E00H06.

Fassett, C.I., Head, James W., Baker, D.M.H., Zuber, M.T., Smith, D.E., Neumann, G.A., Solomon, S.C., Klimczak, C., Strom, R.G., Chapman, C.R., Prockter, L.M., Phillips, R.J., Oberst, J., Preusker, F., 2012b. Large impact basins on Mercury: global distribution, characteristics, and modification history from MESSENGER orbital data. J. Geophys. Res. 117. CiteID E00L08.

Featherstone, W.E., Hirt, C., Kuhn, M., 2013. Band-limited Bouguer gravity identifies new basins on the Moon. J. Geophys. Res. 118, 1397–1413. http://dx.doi.org/10.1002/jgre.20101.

Frey, H.V., 2006. Impact constraints on the age and origin of the lowlands of Mars. Geophys. Res. Lett. 33. http://dx.doi.org/10.1029/2005GL024484.

Frey, H.V., 2008. Ages of very large impact basins on Mars: implications for the late heavy bombardment in the inner Solar System. Geophys. Res. Lett. 35. CiteID L13203.

Frey, H.V., 2012. Preliminary crater retention ages for an expanded inventory of large lunar basins. In: 43rd Lunar and Planetary Science Conference. In: LPI Contrib., vol. 1659. Id. 1852.

Gault, D.E., 1970. Saturation and equilibrium conditions for impact cratering on the lunar surface: criteria and implications. Radio Sci. 5, 273–291.

Gomes, R., Levison, H.F., Tsiganis, K., Morbidelli, A., 2005. Origin of the cataclysmic late heavy bombardment period of the terrestrial planets. Nature 435, 466–469.

Hansen, B.M.S., 2009. Formation of the terrestrial planets from a narrow annulus. Astrophys. J. 703, 1131.

Hartmann, W.K., 1972. Paleocratering of the Moon: review of Post-Apollo data. Astrophys. Space Sci. 17, 48–64.

Hartmann, W.K., 1975. Lunar 'cataclysm' – a misconception. Icarus 24, 181–187.

Hartmann, W.K., 1984. Does crater 'saturation equilibrium' occur in the Solar System? Icarus 60, 56–74.

Hartmann, W.K., 1995. Planetary cratering I: lunar highlands and tests of hypotheses on crater populations. Meteoritics 30, 451–467.

Hartmann, W.K., 2003. Megaregolith evolution and cratering cataclysm models – lunar cataclysm as a misconception (28 years later). Meteorit. Planet. Sci. 38, 579–593.

Hartmann, W.K., Quantin, C., Mangold, N., 2007. Possible long-term decline in impact rates. 2. Lunar impact-melt data regarding impact history. Icarus 186, 11–23.

Head, J.W., Fassett, C.I., Kadish, S.J., Smith, D.E., Zuber, M.T., Neumann, G.A., Mazarico, E., 2010. Global distribution of large lunar craters: implications for resurfacing and impactor populations. Science 329, 1504–1508.

Herrick, R.R., Curran, L.L., Baer, A.T., 2011. A Mariner/MESSENGER global catalog of mercurian craters. Icarus 215, 452.

Humayun, M., Nemchin, A., Zanda, B., Hewins, R.H., Grange, M., Kennedy, A., Lorand, J.-P., Gopel, C., Fieni, C., Pont, S., Deldicque, D., 2013. Origin and age of the earliest Martian crust from meteorite NWA7533. Nature. http://dx.doi.org/10.1038/nature12764.

Ivanov, B.A., 2001. Mars/Moon cratering rate ratio estimates. Space Sci. Rev. 96, 87–104.

Ivanov, B.A., 2006. Earth/Moon impact rate comparison: searching constraints for lunar secondary/primary cratering proportion. Icarus 183, 504.

Kennedy, T., Jourdan, F., Bevan, A.W.R., Mary Gee, M.A., Frew, A., 2013. Impact history of the HED parent body(ies) clarified by new ^{40}Ar/^{39}Ar analyses of four HED meteorites and one anomalous basaltic achondrite. Geochim. Cosmochim. Acta 115, 162–182.

Kleine, T., Touboul, M., Bourdon, B., Nimmo, F., Mezger, K., Palme, H., Jacobsen, S.B., Yin, Q.-Z., Halliday, A.N., 2009. Hf–W chronology of the accretion and early evolution of asteroids and terrestrial planets. Geochim. Cosmochim. Acta 73, 5150.

Lapen, T.J., Righter, M., Brandon, A.D., Debaille, V., Beard, B.L., Shafer, J.T., Peslier, A.H., 2010. A younger age for ALH84001 and its geochemical link to shergottite sources in Mars. Science 328, 347–351.

Le Feuvre, M., Wieczorek, M.A., 2011. Nonuniform cratering of the Moon and a revised crater chronology of the inner Solar System. Icarus 214, 1–20.

Marchi, S., Chapman, C.R., Fassett, C.I., Head, J.W., Bottke, W.F., Strom, R.G., 2013. Global resurfacing of Mercury 4.0–4.1 billion years ago by heavy bombardment and volcanism. Nature 499, 59–61.

Mars Meteorite Compendium, 2006. JSC Publication No. 27672. http://www.curator.jsc.nasa.gov/curator/antmet/mmc/mmc.htm.

Massironi, M., Cremonese, G., Marchi, S., Martellato, E., Mottola, S., Wagner, R.J., 2009. Mercury's geochronology revised by applying Model Production Function to Mariner 10 data: geological implications. Geophys. Res. Lett. 36. CiteID L21204.

Mezger, K., Debaille, V., Kleine, T., 2013. Core formation and mantle differentiation on Mars. Space Sci. Rev. 174, 27–48.

Moore, H.J., Hodges, C.A., Scott, D.H., 1974. Multiringed basins – illustrated by Orientale and associated features. In: Proceedings of the 5th Lunar Science Conference 1. Pergamon Press, Inc., New York, pp. 71–100.

Morbidelli, A., Levison, H.F., Tsiganis, K., Gomes, R., 2005. Chaotic capture of Jupiter's Trojan asteroids in the early Solar System. Nature 435, 466–469.

Morbidelli, A., Marchi, S., Bottke, W.F., Kring, D.A., 2012. A sawtooth-like timeline for the first billion years of lunar bombardment. Earth Planet. Sci. Lett. 355, 144–151.

Neukum, G., et al., 1975. Cratering in the Earth–Moon system: consequences for age determination. In: Proc. Lunar Science Conf., pp. 2597–2620.

Neukum, G., 1983. Meteoritenbombardement und Datierung planetarer Oberflächen. Habilitation dissertation for faculty membership. Univ. of Munich. 186 pp.

Neukum, G., Ivanov, B.A., Hartmann, W.K., 2001a. Cratering records in the inner Solar System in relation to the lunar reference system. Space Sci. Rev. 96, 55–86.

Neukum, G., Oberst, J., Hoffmann, H., Wagner, R., Ivanov, B.A., 2001b. Geologic evolution and cratering history of Mercury. Planet. Space Sci. 49, 1507–1521.

Neumann, G.A., Lemoine, F.G., Mazarico, E., Smith, D.E., Zuber, M.T., Goossens, S., Head, J.W., Andrews-Hanna, J., Torrence, M.H., Miljkovic, K., Wieczorek, M.A.,

2013. The inventory of lunar impact basins from LOLA and GRAIL. Lunar Planet. Sci. Conf. Abstr. 44, 2379.
Nittler, L.R., Starr, R.D., Weider, S.Z., McCoy, T.J., Boynton, W.V., Ebel, D.S., Ernst, C.M., Evans, L.G., Goldsten, J.O., Hamara, D.K., Lawrence, D.J., McNutt, R.L., Schlemm, C.E., Solomon, S.C., Sprague, A.L., 2011. The major-element composition of Mercury's surface from MESSENGER X-ray spectrometry. Science 333, 1847–1850.
Norman, M.D., Borg, L.E., Nyquist, L.E., Bogard, D.D., 2003. Chronology, geochemistry, and petrology of a ferroan noritic anorthosite clast from Descartes breccia 67215: clues to the age, origin, structure, and impact history of the lunar crust. Meteorit. Planet. Sci. 38, 645–661.
Nyquist, L.E., Bansal, B.M., Wiesmann, H., Shih, C.-Y., 1995. "Martians" young and old: Zagami and ALH84001. Lunar Planet. Sci. Conf. Abstr. 26, 1065.
Nyquist, L., Bogard, D., Yamaguchi, A., Shih, C.-Y., Karouji, Y., Ebihara, M., Reese, Y., Garrison, D., McKay, G., Takeda, H., 2006. Feldspathic clasts in Yamato-86032: remnants of the lunar crust with implications for its formation and impact history. Geochim. Cosmochim. Acta 70, 5990–6015.
Öpik, E.J., 1960. The lunar surface as an impact counter. Mon. Not. R. Astron. Soc. 120, 404.
Pieters, C.M., Head, J.W., 2001. Extent and duration of volcanism in the largest/oldest lunar basin. In: American Geophysical Union, Spring Meeting 2001. Abstract #P21A-05.
Richardson, J.E., 2009. Cratering saturation and equilibrium: a new model looks at an old problem. Icarus 204, 697–715.
Ronca, L.B., Basilevsky, A.T., Kryuchkov, V.P., Ivanov, B.A., 1981. Lunar craters evolution and meteoroidal flux in pre-mare and post-mare times. Moon Planets 245, 209–229.
Shearer, C.K., Floss, C., 2000. Evolution of the Moon's mantle and crust as reflected in trace-element microbeam studies of lunar magmatism. In: Canup, R.M., Righter, K. (Eds.), Origin of the Earth and Moon. University of Arizona Press, Tucson, pp. 339–359.
Shih, C.-Y., Nyquist, L.E., Reese, Y., Bischoff, A., 2008. Sm–Nd and Rb–Sr isotopic studies of meteorite Kalahari 009: an old VLT mare basalt. Lunar Planet. Sci. XXXIX. Abstract 2165.
Shoemaker, E.M., Hackman, R.J., Eggleton, R.E., 1963. Interplanetary correlation of geologic time. Adv. Astronaut. Sci. 8, 70–89.
Stöffler, D., Ryder, G., 2001. Stratigraphy and Isotope ages off lunar geological units: chronological standard for the inner Solar System. Space Sci. Rev. 96, 9–54.
Strom, R.G., Malhotra, R., Ito, T., Yoshida, F., Kring, D.A., 2005. The origin of planetary impactors in the inner Solar System. Science 309, 1847–1850.
Tanaka, K.L., Scott, D.H., Greeley, R., 1992. Global stratigraphy. In: Mars, pp. 345–382.
Tera, F., Papanastassiou, D.A., Wasserburg, G.J., 1973. A lunar cataclysm at 3.95 AE and the structure of the lunar crust. Lunar Planet. Sci. IV. Abstract 723.
Tera, F., Papanastassiou, D.A., Wasserburg, G.J., 1974. Isotopic evidence for a terminal lunar cataclysm. Earth Planet. Sci. Lett. 22, 1–21.
Terada, K., Anand, M., Sokol, A.K., Bischoff, A., Sano, Y., 2007. Cryptomare magmatism 4.35 Gyr ago recorded in lunar meteorite Kalahari 009. Nature 450, 849–852.
Thangjam, G., Reddy, V., Corre, L., Nathues, A., Sierks, H., Hiesinger, H., Li, J.-Y., Sanchez, J.A., Russell, C.T., Gaskell, R., Raymond, C., 2013. Lithologic mapping of HED terrains on Vesta using Dawn Framing Camera color data. Meteorit. Planet. Sci. 48 (11), 2199–2210.
Tsiganis, K., Gomes, R., Morbidelli, A., Levison, H.F., 2005. Origin of the orbital architecture of the giant planets of the Solar System. Nature 435, 459–461.
Walsh, K.J., Morbidelli, A., Raymond, S.N., O'Brien, D.P., Mandell, A.M., 2011. A low mass for Mars from Jupiter's early gas-driven migration. Nature 475, 206–209.
Weirich, J.R., Wittmann, A., Isachsen, C.E., Rumble, D., Swindle, T.D., Kring, D.A., 2010. The Ar–Ar age and petrology of Miller Range 05029: evidence for a large impact in the very early Solar System. Meteorit. Planet. Sci. 45, 1868–1888.
Werner, S.C., 2005. Major Aspects of the chronostratigraphy and geologic evolutionary history of Mars. Doctoral Dissertation. Freie Universität Berlin. 252 pp.
Werner, S.C., 2008. The early martian evolution – constraints from basin formation ages. Icarus 195, 45–60.
Werner, S.C., Ivanov, B.A., 2007. Exogenic dynamics, cratering and surface ages. In: Treatise on Geophysics, vol. 10, 2nd edition, pp. 207–242.
Werner, S.C., Tanaka, K.L., 2011. Redefinition of the crater-density and absolute-age boundaries for the chronostratigraphic system of Mars. Icarus 215, 603–607.
Werner, S.C., Morbidelli, A., Quantin, C., Bottke, W.F., Marchi, S., 2011. Timing of the early geological evolution on Moon and Mars. In: EPSC-DPS Joint Meeting 2011, p. 1180.
Werner, S.C., Ody, A., Poulet, F., 2014. The source crater of martian shergottite meteorites. Science 343 (6177), 1343–1346.
Wetherill, G.W., 1975. Late heavy bombardment of the Moon and terrestrial planets. In: Proc. Lunar Sci. Conf., vol. 6, pp. 1539–1561.
Wilhelms, D.E., 1987. The geologic history of the Moon. In: USGS Professional Paper, vol. 1348, p. 295.
Wood, B.J., Halliday, S.L., 2010. The lead isotopic age of the Earth can be explained by core formation alone. Nature 465, 767–770.